Title: Tree height and hydraulic traits shape growth responses across droughts in a temperate broadleaf forest

Authors: Ian R. McGregor[1,2], Ryan Helcoski[1], Norbert Kunert[1,3], Alan J. Tepley[1,4], Erika B. Gonzalez-Akre[1], Valentine Herrmann[1], Joseph Zailaa[1,5], Atticus Stovall[1,6,7], Norman A. Bourg[1], William J. McShea[1], Neil Pederson[8], Lawren Sack[9,10], Kristina J. Anderson-Teixeira[1,3]*

Author Affiliations:

1. Conservation Ecology Center; Smithsonian Conservation Biology Institute; National Zoological Park, Front Royal, VA 22630, USA
2. Center for Geospatial Analytics; North Carolina State University; Raleigh, NC 27607, USA
3. Center for Tropical Forest Science-Forest Global Earth Observatory; Smithsonian Tropical Research Institute; Panama, Republic of Panama
4. Canadian Forest Service, Northern Forestry Centre, Edmonton, Alberta, Canada
5. Biological Sciences Department; California State University; Los Angeles, CA 90032, USA
6. Department of Environmental Sciences, University of Virginia, Charlottesville, VA 22903, USA
7. NASA Goddard Space Flight Center; Greenbelt, MD 20771, USA
8. Harvard Forest, Petersham, MA 01366, USA
9. Department of Ecology and Evolutionary Biology; University of California, Los Angeles; Los Angeles, CA 90095, USA
10. Institute of the Environment and Sustainability; University of California, Los Angeles; Los Angeles, CA 90095, USA

*corresponding author: teixeirak@si.edu; +1 540 635 6546

Text	word count	other	n
Total word count (excluding summary, references and legends)	currently ~5855 (strict limit 6,500)	No. of figures	2 (both colour)
Summary	currently 194 (limit 200)	No. of Tables	5
Introduction	currently ~1468	No of Supporting Information files	6
Materials and Methods	currently ~2162		
Results	currently ~674		
Discussion	currently ~1551 (limit 30% of total (not strict), or 1950 if manuscript reaches word limit)		
Acknowledgements	currently ~124		

Summary

- As climate change is driving increased drought in many forested regions around the world, mechanistic understanding of factors conferring drought resistance in trees is increasingly important. The dendrochronological record provides a window through which we can understand how tree size and species' traits shape tree growth responses during droughts.
- We analyzed tree-ring records for twelve species of an oak-hickory forest - representing 97% of woody productivity - in the 25.6-ha ForestGEO plot in Virginia (USA) to determine how tree size, microenvironment characteristics, and species' traits shaped drought responses across the three strongest regional droughts over a 60-year period (1950 - 2009).
- Individual-level drought resistance decreased with tree height, which was the dominant size-related variable affecting drought response. Resistance was greater among species whose leaves lost turgor (wilted) at more negative water potentials, and whose leaves experienced less shrinkage upon desiccation. However, there was substantial variation in the best predictor variables across the three drought periods.
- We conclude that hydraulic traits and tree height influence growth responses during drought, and can explain variation in the tree ring record spanning historical droughts. Thus, these factors can be useful for predicting future drought responses under climate change.

Key words: annual growth; canopy position; drought; Forest Global Earth Observatory (ForestGEO); leaf hydraulic traits; temperate broadleaf deciduous forest; tree height; tree-ring

Introduction

Forests globally play a critical role in climate regulation (Bonan, 2008), yet there remains enormous uncertainty as to how the terrestrial carbon (C) sink, which is dominated by forests, will respond to climate change (Friedlingstein et al., 2006). An important aspect of this uncertainty lies with physiological responses of trees to drought (Kennedy et al., 2019). In many forested regions around the world, the risk of severe drought is increasing (Trenberth et al., 2014); Dai et al. 2018), often despite increasing precipitation (Intergovernmental Panel on Climate Change, 2015). Droughts, exasperated by climate change, have been affecting forests worldwide (Allen et al., 2010), and are expected to continue as one of the most important drivers of forest change in the future (Allen et al., 2015). Understanding and modeling forest responses to drought requires elucidation of how tree size, microenvironment, and species' traits jointly influence individual-level drought resistance, and the extent to which their influence is consistent across droughts. However, it has proved difficult to resolve factors affecting tree growth during drought with available forest census data, which only rarely captures extreme drought, and with tree-ring records, which rarely represent many species and size classes at a single site and are not necessarily associated with ecological data. The aim of this study was to pair tree-ring and forest plot data to test how tree size and traits shaped growth responses to historical droughts.

One fundamental question regarding forest responses to drought is what drives the observed tendency for large trees to be more affected by drought. Greater growth reductions for larger trees was first shown on a global scale by Bennett et al. (2015), and numerous subsequent studies have reinforced this finding (*e.g.*, Stovall et al. (2019); Hacket-Pain et al. (2016)). It has yet to be resolved which of several potential underlying mechanisms drive this pattern. First, tree height may be a primary driver. Taller trees have a greater biophysical challenge of lifting water greater distances against the effects of gravity and friction (McDowell et al., 2011; McDowell and Allen, 2015; Ryan et al., 2006; Couvreur et al., 2018). Vertical gradients in stem and leaf traits–including smaller and thicker leaves (higher LMA), more negative $P50$, and lower hydraulic conductivity at greater heights (Couvreur et al., 2018; Koike et al., 2001; McDowell et al., 2011)–make it biophysically possible for trees to become tall (Couvreur et al., 2018). Meanwhile, tall trees require greater hydraulic efficiency, such that xylem conduit diameter increases with tree height within and across species (Olson et al., 2018; Liu et al., 2019), making large trees more vulnerable to embolism during drought (Olson et al., 2018). Traits conducive to efficient water transport may also lead to poor ability to recover from or re-route water around embolisms (Roskilly et al., 2019). Second, larger trees may have lower drought resistance because they tend to have more exposed crown positions, where they are exposed to higher solar radiation, greater wind speeds, and lower humidity (e.g., Koike et al. (2001); Kunert et al. (2017)). Subcanopy trees tend to fare better specifically due to the benefits of a buffered environment (Pretzsch et al., 2018). Potentially counteracting the biophysical challenges faced by large trees, their larger root systems confer a potential advantage in terms of allowing greater access to water; however, it appears that this effect is usually insufficient to offset the costs of height and/or crown exposure. A final mechanism that could mediate tree size-related responses to drought is how species, and their associated hydraulic traits, are distributed with respect to size (Meakem et al., 2018; Liu et al., 2019). Understanding the mechanisms driving the greater growth reductions of larger trees during drought will require sorting out the interactive effects of height, canopy position, root water access, and species' traits.

Debates have also arisen regarding the traits that would influence tree growth responses to drought. Commonly-measured traits including wood density (WD) and leaf mass per area (LMA) have been linked to

drought responses in some temperate deciduous forests (Abrams, 1990; Guerfel et al., 2009; Hoffmann et al., 2011) and other forest biomes around the world (Greenwood et al., 2017). However, in other cases these traits have failed to link to drought tolerance (Maréchaux et al. 2019), and the direction of response is not always consistent; for instance, higher WD has been associated with greater drought resistance at a global scale (Greenwood et al., 2017) but correlated negatively with tree performance during drought in a broadleaf deciduous forest in the southeastern United States (Hoffmann et al., 2011). Thus, their role may be due to indirect correlations with other traits within life-history strategies (Hoffmann et al., 2011). Recent work has shown a great potential for hydraulic traits to predict growth and mortality responses. Hydraulic traits including water potentials at which percent loss conductivity surpass a certain threshold ($P50$, $P80$, $P88$) and hydraulic safety margin have enabled prediction of drought performance (Anderegg et al., 2018) but are time-consuming to measure and therefore infeasible for predicting or modeling drought responses in highly diverse forests (*e.g.*, in the tropics). More rapidly measurable leaf hydraulic traits with direct linkage to plant hydraulic function are emerging with potential to explain greater variation in plant distribution and function than the more commonly-measured WD and LMA (Medeiros et al., 2019). These include leaf area shrinkage upon desiccation (PLA_{dry}; (Scoffoni et al., 2014)) and the leaf water potential at turgor loss point (π_{tlp}), *i.e.,* the water potential at which leaf wilting occurs (Bartlett et al., 2016). The abilities of both PLA_{dry} and π_{tlp} to explain tree performance under drought remains untested.

The long time frame captured in tree-ring data enables us to address the question of whether tree size and species' traits have similar influence across different drought events, or whether that influence is more strongly predicted by community-level responses to variable drought severity, duration, and timing based on tree size and traits. Tree growth responses vary with drought characteristics such as timing and atmospheric demand (D'Orangeville et al., 2018), but the question of how tree size and species' traits impact growth responses across droughts still remains. While tree-ring studies provide long-term records of tree responses to multiple droughts (e.g., Lloret et al. (2011); D'Orangeville et al. (2018)), they generally focus on species-level responses, and do not consider the roles of tree size and microenvironment. The ecological field-baesd studies that have shaped our understanding of the role of tree size and microenvironment in forest drought responses generally examine only a single drought and tend to focus disproportionately on the most extreme droughts with dramatic impacts (*e.g.*, Allen et al. (2010); Bennett et al. (2015); Stovall et al. (2019); Anderegg et al. (2016)). Thus, our knowledge of forest responses to more modest but frequent droughts - e.g., those with historical return intervals on the order of one to two decades - remains limited. There is evidence that the degree to which larger trees are more impacted by drought increases with the severity of drought conditions (Bennett et al., 2015; Stovall et al., 2019), so the influence of tree size may be less in weaker–but more common–droughts. Thus, while we expect many of the mechanisms shaping drought responses to be universal, we have little understanding of how tree size and traits interact with drought characteristics, and the extent to which their influence is consistent across droughts.

To yield functional understanding of how tree size, microenvironment characteristics, and species' traits collectively shape drought responses, we test a series of hypotheses and associated specific predictions (Table 1) based on the combination of tree-ring records from three droughts (1966, 1977, 1999), species functional and hydraulic trait measurements, and forest census data from a 25.6-ha ForestGEO plot in Virginia (USA). First, we focus on the role of tree size and its interaction with microenvironment. We test whether, consistent with most forests globally, larger-diameter trees tend to have lower drought resistance (Rt) in this forest, which is in a region (eastern North America) represented by only two studies in Bennett et al. (2015).

We then test hypotheses designed to disentangle the relative importance of tree height; crown exposure; and soil water availability, which should be greater for larger trees in dry but not in perpetually wet microsites. Second, we focus on the role of species' functional and hydraulic traits, testing the hypothesis that species' traits—particularly leaf hydraulic traits—predict Rt. We test predictions that drought resistance is correlated with wood density–either postively (Greenwood et al., 2017) or negatively (Hoffmann et al., 2011)– and positively correlated with specific leaf area, but that hydraulic leaf traits including PLA_{dry} and π_{tlp} are better predictors. We expect that ring-porous species would have greater drought resistance than semi-ring and diffuse-porous species, as has been previously observed (Kannenberg et al., 2019; Elliott et al., 2015; Friedrichs et al., 2009).

Materials and Methods

Study site

Research was conducted at the 25.6 ha ForestGEO (Forest Global Earth Observatory) study plot at the Smithsonian Conservation Biology Institute (SCBI) in Virginia, USA (38°53'36.6"N, 78°08'43.4"W) (Bourg et al., 2013; **?**). SCBI is located in the central Appalachian Mountains at the northern edge of Shenandoah National Park. Elevations range from 273-338m above sea level with a topographic relief of 65m (Bourg et al., 2013). Climate is humid temperate, with mean annual temperature of 12.7°C and precipitation of 1005 mm during our study period (1960-2009; source: CRU TS v.4.01; Harris et al. (2014)). Dominant tree taxa within this secondary forest include *Liriodendron tulipifera*, oaks (*Quercus* spp.), and hickories (*Carya* spp.).

Data collection and preparation

All analysis beyond basic data collection was performed using R version 3.5.3 (R Core Team, 2019).

Within or just outside the ForestGEO plot, we collected data on a suite of variables including tree size, microenvironment characteristics, and species traits (Table 2). The SCBI ForestGEO plot was censused in 2008, 2013, and 2018 following standard ForestGEO protocols, whereby all free-standing woody stems $\geq$ 1cm diameter at breast height (DBH) were mapped, tagged, measured at DBH, and identified to species (Condit, 1998). From this census data, we used measurements of DBH from 2008 to calculate historical DBH and data for all stems $\geq$ 10cm to analyze functional trait composition relative to tree height (all analyses described below). Census data, which were last updated in 2019, are available through the ForestGEO data portal (www.forestgeo.si.edu).

We analyzed tree-ring data (cambial growth increment) from 571 trees representing the twelve species contributing most to woody aboveground net primary productivity ($ANPP_{stem}$), which together comprised 97% of study plot $ANPP_{stem}$ between 2008 and 2013 (Helcoski et al., 2019) (Figure S1). Cores were collected within the ForestGEO plot at breast height (1.3m) in 2010-2011 or 2016-2017 using a 5mm increment borer. In 2010-2011, cores were collected from randomly selected live trees of species with at least 30 individuals $\geq$ 10cm DBH (Bourg et al., 2013). In 2016-2017, cores were collected from all trees found dead in the annual mortality census (Gonzalez-Akre et al., 2016). Cores were sanded, measured, and cross-dated using standard procedures, as detailed in (Helcoski et al., 2019). The resulting chronologies were published in association with Helcoski et al. (2019) (DOI: 10.5281/ zenodo.2649302).

For each cored tree, we combined tree-ring records and allometric equations of bark thickness to retroactively calculate DBH for the years 1950-2009. Prior DBH was estimated using the following equation:

$$DBH_Y = DBH_{2008} - 2 * \left[\sum_{year=Y}^{2008} (r_{ring,Y} : r_{ring,2008}) - r_{bark,Y} + r_{bark,2008} \right]$$

Here, Y denotes the year of interest, r_{ring} denotes ring width derived from cores, and r_{bark} denotes bark thickness. Bark thickness was estimated from species-specific allometries based on the bark thickness data from the site (Anderson-Teixeira et al., 2015). Specifically, we used linear regression equations on log-transformed data to relate bark thickness to diameter inside bark from 2008 data (Table S1), which were then used to determine bark thickness in the retroactive calculation of DBH.

Height measurements (H, n=1518 trees) were taken by several researchers between 2012 to 2019. Measurement methods included manual (Stovall et al., 2018a; NEON, 2018), digital rangefinders (Anderson-Teixeira et al., 2015; NEON, 2018), and automatic, ground-based LiDAR (Stovall et al., 2018b). Rangefinders used either the tangent method (Impulse 200LR, TruPulse 360R) or the sine method (Nikon ForestryPro) for calculating heights. Both methods are associated with some error (Larjavaara and Muller-Landau, 2013), but in this instance there was no clear advantage of one or the other. Measurements from the National Ecological Observatory Network (NEON) were collected nearby the ForestGEO plot following standard NEON protocol, whereby vegetation of short stature was measured with a collapsible measurement rod, and taller trees with a rangefinder (NEON, 2018). Species-specific height allometries were developed (Table S2) using logarithmic regression ($ln[H]$). For species with insufficient height data to create reliable species-specific allometries, heights were calculated from an equation developed using all height measurements.

Crown position (CP)–a categorical variable including dominant, co-dominant, intermediate, and suppressed–was recorded for all cored trees that remained standing during the growing season of 2018 following the protocol of Jennings et al. (1999). While some trees undoubtedly changed position in the 52 years between the 1966 drought and our observations in 2018, in this case the bias would be unlikely to result in false acceptance of our hypothesis (i.e., type I error unlikely; type II error possible). An analysis of crown position relative to height (Fig. 2d) and height changes since the beginning of the study period indicated that changes were fairly small relative to differences among canopy positions (Fig. S3), with average tree height growth confined to ~0.82m from 1966 to 1977, ~1.45m from 1977 to 1999, and ~1.97m from 1999 to 2018. However, dominant and co-dominant trees were similar in height (Figs. 2d, S3).

Topographic wetness index (TWI) was calculated using the dynatopmodel package in R (Figure S1) (**?**). Originally developed by Beven and Kirkby (1979), TWI was part of a hydrological run-off model and has since been used for a number of purposes in hydrology and ecology (Sørensen et al., 2006). TWI calculation depends on an input of a digital elevation model (DEM), and from this yields a quantitative assessment defined by how "wet" an area is, based on areas where run-off is more likely. From our observations in the plot, the calculation of TWI performed comparatively better at categorizing wet areas than the calculation of a distance matrix from a stream shapefile.

Hydraulic traits were collected at SCBI (Table 3) in August 2018. We sampled small sun-exposed branches within eight meters of the ground from three individuals of each species in and around the ForestGEO plot. Sampled branches were re-cut under water at least two nodes above the original cut and re-hydrated overnight in covered buckets (opaque plastic bags) before measurements were taken. Rehydrated leaves taken towards the apical end of the branch (n=3 per individual: small, medium, and large) were scanned, weighed,

dried at 60° C for $\geq$ 48 hours, and then re-scanned and weighed. Leaf area was calculated from scanned images using the LeafArea R package (**?**). LMA was calculated as the ratio of leaf dry mass to fresh area. PLA_{dry} was calculated as the percent loss of area between fresh and dry leaves. WD was calculated for ~1cm diameter stem samples (bark and pith removed) as the ratio of dry weight to volume, which was estimated using Archimedes' displacement. We used the rapid determination method of Bartlett et al. (2012) to estimate water potential at turgor loss point (π_{tlp}). Briefly, two 4mm diameter leaf discs were cut from each leaf, tightly wrapped in foil, submerged in liquid nitrogen, perforated 10-15 times with a dissection needle, and then measured using a vapour pressure osmometer (VAPRO 5520, Wescor, Logan, UT, USA). Osmotic potential (π_{osm}) given by the osmometer was used to estimate (π_{tlp}) using the equation $\pi_{tlp} = 0.832\pi_{osm}^{-0.631}$ (Bartlett et al., 2012).

To characterize how environmental conditions vary with height, data were obtained from the National Ecological Observation Network (NEON) tower located <1km from the study area. We used data on wind speed, relative humidity, and air temperature, all measured over a vertical profile spanning from 7.2 m height to above the top of the tree canopy (31.0 or 51.8m, depending on censor), for the years 2016-2018 (**?**). After filtering for missing and outlier values, the data were consolidated to represent the mean values per sensor height per day. The range of these means were then aggregated at a month scale.

Identification of drought years

We identified droughts within the time period 1950-2009, defining drought (Slette et al., 2019) as events with both anomalously dry peak growing season climatic conditions and widespread reductions in tree growth. Simultaneous consideration of both meteorological conditions and tree growth ensured that drought was the primary driver of observed growth declines and that our focus remained on droughts that substantially impacted the forest community.

We identified the years with driest conditions during May-August (MJJA), which stood out in the analysis of Helcoski et al. (2019) as the current-year months to which annual growth was most sensitive for trees at this site. We considered two metrics of moisture deficit: NOAA Divisional Data's Palmer Drought Severity Index (PDSI) and the difference between monthly potential evapotranspiration (PET) and precipitation (PRE). These data were obtained from the ForestGEO Climate Data Portal (https://github.com/forestgeo/Climate) in August 2018, with monthly PET and PRE sourced from Climatic Research Unit high-resolution gridded dataset (CRU TS v.4.01; Harris et al. (2014)). The driest years were identified through ranking mean MJJA $PET - PRE$ or $PDSI$ for the time period from driest to wettest. Three of the five years between 1950 and 2009 with greatest moisture deficit ($PET - PRE$) during MJJA consistently ranked as the three driest in terms of $PDSI$: 1966, 1977, and 1999, which had mean MJJA $PET - PRE$ of 83, 87, and 80 mm mo-1, respectively (Table S3). The years 1964 and 2007 also ranked among the five lowest $PET - PRE$ (84 and 82 mm mo-1, respectively), but were not among the lowest in terms of PDSI and were thus not identified as candidate years for inclusion as top drought years (Table S3).

We defined years with widespread growth reduction ("pointer years") as those where >25% of the cored trees experienced >30% reduction in basal area increment (BAI) relative to the previous 5 years, following the drought resistance (Rt) metric of (Lloret et al., 2011). Rt values <1 indicate growth reductions, whereas values >1.0 indicate increased growth. Pointer years were identified using the pointRes package (**?**) in R. Four years met our criteria: 1966, 1977, 1991, and 1999. We excluded 1991 (26.5% of trees experienced >30% growth reduction, mean resistance= -13.8%) because this year was not identified as among the driest

of the time period (Table S3). Rather, the severity of growth reduction may be explained in part by defoliation from gypsy moths (*Lymantria dispar* L.) from approximately 1988-1995, which strongly impacted *Quercus* spp. (Twery, 1991).

Together, these criteria identified three drought years: 1966, 1977, and 1999 (Figs. 1, S2, Table S3). The droughts differed in intensity and prior onset (Fig. S2, Table S3). The 1966 drought was preceded by two years of moderate drought during the growing season and severe to extreme drought starting the previous fall and in August reached the minimum growing season $PDSI$ (-4.82) among of any of the three droughts. The 1977 drought was the least intense throughout the growing season, and was preceded by 2.5 years of near-normal conditions, making it the mildest of the three droughts. The 1999 drought was preceded by wetter than average conditions until the previous June, but reached the lowest PDSI during May-July.

Statistical Analysis

For each drought period, we calculated drought resistance (Rt) as the ratio of BAI during drought to the mean BAI over the five years preceding the drought (Lloret et al., 2011). Thus, $Rt<1$ indicates reduced growth under drought. Analyses focused on testing the predictions presented in Table 1, with Rt as the response variable. The general statistical model for hypothesis testing was a mixed effects model (lme4 package from **?**) with Rt as the response variable, tree nested within species as a random effect, and one or more independent variables as fixed effects. We used AICc (AICcmodavg package from **?**) to assess model selection, and conditional/marginal R-squared to assess model fit.

Models were run for all drought years combined (with year as a fixed effect) and for each drought year independently. In order to determine the relative importance of the traits alone, we first tested the predictor variables independently against both height and Rt given height's substantial influence. Variables were considered to have significant influence on Rt when AICc was reduced by ≥ 2 relative to the corresponding null model lacking that variable (Table 4).

We then determined the best full models for predicting Rt for each individual drought year and for all years combined. Candidate variables were selected, based on the single-variable tests, as those whose addition to a corresponding null model improved fit (at dAICc ≥ 1.0) in at least one drought (Table 4). We compared models with all possible combinations of candidate variables and identified the full set of models within dAICc=1 of the very top model (that with lowest AICc), henceforth referred to as "full models". When a variable appeared in all top models and the sign of the coefficient was consistent across models, this was counted as support for/ rejection of the associated prediction by the full models. If the variable appeared in only some of the models, we considered this partial support/rejection.

All data, code, and results are available through the SCBI-ForestGEO organization on GitHub (https://github.com/SCBI- ForestGEO: SCBI-ForestGEO-Data and McGregor_climate-sensitivity-variation repositories), with static versions corresponding to data and analyses presented here archived in Zenodo (DOIs: 10.5281/zenodo.3604993 and [TBD], respectively).

Results

Community-level drought responses

Community-level tree growth responses to all three droughts were modest, with mean Rt values of 0.86, 0.84, and 0.86 for 1966, 1977, and 1999 droughts, respectively (Fig. 1b). In each drought, roughly 30% of the cored

trees experienced ≥ 30% growth reductions ($Rt \leq 0.7$): 29% in 1966, 32% in 1977, and 27% in 1999. However, some individuals exhibited increased growth: ($Rt > 1.0$): 26% in 1966, 22% in 1977, and 26% in 1999.

Tree size, microenvironment, and drought resistance

Larger-diameter trees showed greater reductions in growth during drought, although there was no significant effect during 1977 or 1999 individually (Tables 1, 4). The same held true for $ln[H]$ in single-variable tests (Tables 1, 4). When combined with other predictor variables in the full models, $ln[H]$ appeared, with negative coefficient, in all full models for the three droughts combined, in the 1966 model, and in one of the two 1999 models (Tables 1, 5).

Crown position varied as expected with H (dominant > co-dominant > intermediate > suppressed), but with substantial variation (Fig. 2d). Crown position was a much poorer predictor of Rt than was H in the single-variable tests (Table 4), lending little overall support to the hypothesis that trees with more exposed crowns have lower Rt (Table 1). When considered alone, CP had a significant response only in the 1966 drought, during which trees with dominant CP had the lowest Rt. When H was included in the model, CP was a significant predictor in the 1999 drought, with lowest Rt for suppressed and then intermediate trees. Crown position was included in some of the full models (Table 5). In 1977, where H was not included in the full model, dominant trees had the lowest Rt, and suppressed the highest. In contrast, in full models including both H and CP (all droughts and 1999), the lowest Rt was in suppressed, followed by intermediate, trees.

In the non-drought years for which we have vertical profiles in climate data (2016-2018), taller trees–or those in dominant crown positions– were generally exposed to higher evaporative demand during the peak growing season months (May-August; Fig. 2). Specifically, maximum daily wind speeds were significantly higher above the top of the canopy (40-50m) than within and below (10-30m) (Fig. 2a). Relative humidity was also somewhat lower during June-August, ranging from ~50-80% above the canopy and ~60-90% in the understory (Fig. 2b). Air temperature did not vary across the vertical profile (Fig. 2c).

Resistance was negatively correlated with $ln[TWI]$ (Tables 4-5), negating the idea that trees in moist microsites would be less affected by drought. Nevertheless, we tested for a negative $ln[H] * ln[TWI]$ interaction, which could indicate that smaller trees (with smaller rooting volume) are more susceptible to drought in drier microenvironments with a deeper water table. This hypothesis was rejected; the $ln[H] * ln[TWI]$ interaction was never significant and had a consistently positive coefficient (Table 4).

Species' traits and drought resistance

Hydraulic traits, including XP, PLA_{dry}, and π_{tlp}, were linked to drought responses (Tables 1,4,5). In the single-variable tests, LMA and WD never significantly associated with Rt (Table 4) and were excluded from the full models. In contrast, XP, PLA_{dry}, and π_{tlp} all explained modest amounts of variation (dAIC > 1.0) in at least one drought (Table 4). PLA_{dry} was a strong predictor for the 1966 drought and all droughts combined, with consistently negative coefficients (Table 4). Similarly, PLA_{dry} was consistently included, with negative coefficient, in full models for the three droughts combined and for the 1966 and 1977 droughts individually (Table 5). π_{tlp} did not come out significant in any single-variable tests; however, coefficients were consistently negative (Table 4) and π_{tlp} was included in the top full model for all droughts combined and for the 1977 and 1999 droughts individually (Table 5). Xylem porosity was not significant for all droughts combined and had contrasting effects in the individual droughts: whereas ring-porous species had

higher Rt than diffuse- and semi-ring- porous species in the 1966 and 1999 droughts, they had lower Rt in 1977 (Tables 4,5).

Discussion

Tree size, microenvironment, and hydraulic traits shaped tree growth responses across three droughts (Table 1). The greater susceptibility of larger trees to drought, similar to forests worldwide (Bennett et al., 2015), was driven primarily by their height (Liu and Muller, 1993; Stovall et al., 2019). There was a marginal additional effect of crown exposure, with a tendency for lowest Rt among the most exposed (dominant) and suppressed trees. There was no evidence that soil water availability increased drought resistance; in contrast, trees in wetter topographic positions had lower Rt (consistent with Zuleta et al. (2017); Stovall et al. (2019)), and the larger potential rooting volume of large trees provided no advantage in the drier microenvironments. The negative effect of height on Rt held when also accounting for species' traits. Drought sensitivity was not consistently linked to species' LMA, WD, or xylem architecture, but was negatively correlated with the leaf hydraulic traits (PLA_{dry}, π_{tlp}) in the top overall model and the top models for two of the three individual droughts (Scoffoni et al., 2014; Bartlett et al., 2016; Medeiros et al., 2019). This is a novel finding in that PLA_{dry} and π_{tlp} have not previously been linked to drought growth responses. The direction of responses was mostly consistent across droughts, supporting the conclusion that they were driven by fundamental physiological mechanisms. However, the strengths of each predictor varied across droughts (Tables 4-5), indicating that drought characteristics interact with tree size, microenvironment, and traits to shape which individuals are most affected. These findings significantly advance our knowledge of the factors that confer vulnerability or resistance on trees during drought.

The droughts considered here were of a magnitude that has occurred with an average frequency of approximately one per 10-15 years (Fig. 1a, Helcoski et al. (2019)) and had modest impacts on tree growth (Fig. 1b). These droughts were classified as severe (1977) or extreme (1966, 1999) according to the PDSI metric and have been linked to tree mortality in the eastern United States (Druckenbrod et al., 2019); however, extreme, multiannual droughts ("megadroughts") of the type that have triggered massive tree die-off in other regions (e.g., Allen et al. (2010); Stovall et al. (2019)) have not occurred in the Eastern United States within the past several decades (Clark et al., 2016). Of the droughts considered here, the 1966 drought, which was preceded by two years of dry conditions (Fig. S2), severely stressed a larger portion of trees (Fig. 1b). It may be notable that the tendency for large trees to have lowest resistance was most pronounced in this drought, consistent with other findings that this tendency increases with drought strength (Bennett et al., 2015; Stovall et al., 2019). Across all three droughts, the majority of trees experienced reduced growth, but a substantial portion had increased growth (Fig. 1b), potentially due to decreased leaf area of competitors during the drought. It is likely because of the moderate impact of these droughts, along with other factors influencing tree growth, that our best models characterize only a modest amount of variation: 11-13% for all droughts combined, and 21-26% for each individual drought (Table 5).

Our analysis indicates that tree height has a stronger influence on drought response than does canopy position (Tables 1,4,5). This is consistent with, and reinforces, previous findings that biophysical constraints make it impossible for trees to efficiently transport water to great heights and simultaneously maintain strong resistance and resilience to drought-induced embolism (Olson et al., 2018; Couvreur et al., 2018; Roskilly et al., 2019). However, this result must be interpreted with some caution, given that collinearity between the two variables (Fig. 2d) makes it impossible to confidently partition causality. Taller trees are

more likely to be in dominant canopy positions (Fig. 2d) and, largely as a consequence of their position relative to others, face different microenvironments (Fig. 2a-b). Even under non-drought conditions, evaporative demand and maximum leaf temperatures increase with tree height (Smith and Nobel, 1977; Bretfeld et al., 2018; Kunert et al., 2017), and such conditions would incur extra stress during drought, when solar radiation tends to be higher and less water is available for evaporative cooling of the leaves. However, some decoupling between height and canopy position is introduced by the configuration of neighboring trees (Fig. 2d) (Muller-Landau et al., 2006), and height was an overall stronger predictor of drought response than crown position (Tables 1,4,5).

Our analysis has the limitation that canopy positions were recorded in 2018, as opposed to the years of the droughts. However, because trees would generally advance towards more dominant positions as they grow and as neighbors die, changing canopy positions would bias against the acceptance of our hypothesis. The implication is that dominant crown positions did have a marginally negative influence on Rt, which makes sense in light of the vertical environmental gradients described above and agrees with previous studies showing greater drought sensitivity in more exposed trees (Suarez et al., 2004; Scharnweber et al., 2019). It is safe to assume that currently suppressed trees have always been in the understory, and their relatively low Rt (after accounting for height effects) is real, perhaps as a result of competition (*Sohn et al. 2016*). The observed height-sensitivity of Rt, together with the lack of advantage to large stature in drier topographic positions, agrees with the concept that physiological limitations to transpiration under drought shift from soil water availability to the plant-atmosphere interface as forests age (Bretfeld et al., 2018), such that tall, dominant trees are the most sensitive in mature forests. Additional research comparing drought responses of young and old forest stands, along with short and tall isolated trees, would be valuable for more clearly disentangling the roles of tree height and crown exposure.

The development of tree-ring chronologies for the twelve most dominant tree species at our site (Helcoski et al., 2019; Bourg et al., 2013) gave us the sample size to compare historical drought responses across species and associated traits at a single site (see also Elliott et al., 2015). Concerted measurement of leaf hydraulic traits of emerging importance (Scoffoni et al., 2014; Bartlett et al., 2016; Medeiros et al., 2019) allowed novel insights into the role of hydraulic traits in shaping drought response. The finding that PLA_{dry} and π_{tlp} can be useful for predicting drought responses of tree growth (Tables 1,4,5) is both novel and consistent with previous studies linking these traits to habitat and drought tolerance. Previous studies have demonstrated that π_{tlp} and PLA_{dry} are physiologically meaningful traits linked to species distribution along moisture gradients (Medeiros et al., 2019; Simeone et al., 2019; Maréchaux et al., 2015) (*Rosas et al. 2019, DOI: 10.1111/nph.15684*, Fletcher et al. 2018), and our findings indicate that these traits also influence drought responses. Furthermore, the observed linkage of π_{tlp} to Rt in this forest aligns with observations in the Amazon that π_{tlp} is higher in drought-intolerant that drought-tolerant plant functional types and adds support to the idea that this trait is useful for categorizing and representing species' drought responses in models (*Powell et al. 2016, DOI: 10.1111/gcb.13731*). Because both PLA_{dry} and π_{tlp}, which can be measured relatively easily (Bartlett et al., 2012; Scoffoni et al., 2014), they hold promise for predicting drought growth responses across species. The importance of linking species' traits to drought responses increases with tree species diversity; whereas it is feasible to study drought responses for all dominant species in most boreal and temperate forests (e.g., this study), this becomes difficult to impossible for species that don't form annual rings, and for diverse tropical forests. Although progress is being made for the tropics (Schöngart et al., 2017), a full linkage hydraulic traits to drought responses would be invaluable for

forecasting how little-known species and whole forests will respond to future droughts (*Powell et al. 2016, DOI: 10.1111/gcb.13731*).

As climate change drives increasing drought in many of the world's forests (Trenberth et al., 2014; Intergovernmental Panel on Climate Change, 2015), the fate of forests and their climate feedbacks will be shaped by the biophysical and physiological drivers observed here. Large trees have been disproportionately impacted in forests around the world (Bennett et al., 2015; Stovall et al., 2019), and we show, at least at this site, that this is primarily driven by their height with some contributions from canopy position. The distinction is important because it suggests that height *per se* makes trees vulnerable, even if their crowns are somewhat protected by neighbors, whereas solitary trees or the dominant trees in young regrowth forests should be less vulnerable. This would suggest that, all else being equal, mature forests would be more vulnerable to drought than young forests with short trees; however, root water access may limit the young forests (Bretfeld et al., 2018), and species traits often shift as forests age. Early successional species at our site (*Liriodendron tulipifera*, *Quercus spp.*, *Fraxinus americana*) display a mix of traits conferring drought tolerance and resistance (Table 3), and further research on how hydraulic traits and drought vulnerability change over the course of succession would be valuable for addressing how drought tolerance changes as forests age (e.g. Rodríguez-Catón et al., 2015). In the meantime, the results of this study advance our knowledge of the factors conferring drought vulnerability and resistance in a mature forest, opening the door for more accurate forecasting of forest responses to future drought.

Acknowledgements

We especially thank the numerous researchers who helped to collect the data used here, in particular Jennifer C. McGarvey, Jonathan R. Thomspon, and Victoria Meakem for original collection and processing of cores. Thanks also to Camila Medeiros for guidance on hydraulic and functional trait measurements, Edward Brzostek's lab for collaboration on leaf sampling, and Maya Prestipino for data collection. Funding for the establishment of the SCBI ForestGEO Large Forest Dynamics Plot was provided by the Smithsonian-led Forest Global Earth Observatory (ForestGEO), the Smithsonian Institution, and the HSBC Climate Partnership. This study was funded by ForestGEO, a Virginia Native Plant Society grant to KAT and AJT, and support from the Harvard Forest and National Science Foundation which supports the PalEON project (NSF EF-1241930) for NP.

Author Contribution

KAT, IM, and AT designed the research. Tree-ring chronologies were developed by RH under guidance of AT and NP. Trait data was collected by IM, JZ under guidance of NK and LS. Other plot data were collected by IM, AS, EGA, and NB under guidance of EGA and WM. Data analyses were performed by IM under guidance of KAT and VH. KAT and IM interpreted the results. IM and KAT wrote the first draft of manuscript, and all authors contributed to revisions.

References

Abrams, M. D. (1990). Adaptations and responses to drought in Quercus species of North America. *Tree Physiology*, 7(1-2-3-4):227–238.

Allen, C. D., Breshears, D. D., and McDowell, N. G. (2015). On underestimation of global vulnerability to tree mortality and forest die-off from hotter drought in the Anthropocene. *Ecosphere*, 6(8):art129.

Allen, C. D., Macalady, A. K., Chenchouni, H., Bachelet, D., McDowell, N., Vennetier, M., Kitzberger, T., Rigling, A., Breshears, D. D., Hogg, E. H. T., Gonzalez, P., Fensham, R., Zhang, Z., Castro, J., Demidova, N., Lim, J.-H., Allard, G., Running, S. W., Semerci, A., and Cobb, N. (2010). A global overview of drought and heat-induced tree mortality reveals emerging climate change risks for forests. *Forest Ecology and Management*, 259(4):660–684.

Anderegg, W. R. L., Klein, T., Bartlett, M., Sack, L., Pellegrini, A. F. A., Choat, B., and Jansen, S. (2016). Meta-analysis reveals that hydraulic traits explain cross-species patterns of drought-induced tree mortality across the globe. *Proceedings of the National Academy of Sciences*, 113(18):5024–5029.

Anderegg, W. R. L., Konings, A. G., Trugman, A. T., Yu, K., Bowling, D. R., Gabbitas, R., Karp, D. S., Pacala, S., Sperry, J. S., Sulman, B. N., and Zenes, N. (2018). Hydraulic diversity of forests regulates ecosystem resilience during drought. *Nature*, 561(7724):538–541.

Anderson-Teixeira, K. J., McGarvey, J. C., Muller-Landau, H. C., Park, J. Y., Gonzalez-Akre, E. B., Herrmann, V., Bennett, A. C., So, C. V., Bourg, N. A., Thompson, J. R., McMahon, S. M., and McShea, W. J. (2015). Size-related scaling of tree form and function in a mixed-age forest. *Functional Ecology*, 29(12):1587–1602.

Bartlett, M. K., Klein, T., Jansen, S., Choat, B., and Sack, L. (2016). The correlations and sequence of plant stomatal, hydraulic, and wilting responses to drought. *Proceedings of the National Academy of Sciences*, 113(46):13098–13103.

Bartlett, M. K., Scoffoni, C., Ardy, R., Zhang, Y., Sun, S., Cao, K., and Sack, L. (2012). Rapid determination of comparative drought tolerance traits: using an osmometer to predict turgor loss point. *Methods in Ecology and Evolution*, 3(5):880–888.

Bennett, A. C., McDowell, N. G., Allen, C. D., and Anderson-Teixeira, K. J. (2015). Larger trees suffer most during drought in forests worldwide. *Nature Plants*, 1(10):15139.

Beven, K. J. and Kirkby, M. J. (1979). A physically based, variable contributing area model of basin hydrology / Un modèle à base physique de zone d'appel variable de l'hydrologie du bassin versant. *Hydrological Sciences Bulletin*, 24(1):43–69.

Bonan, G. B. (2008). Forests and Climate Change: Forcings, Feedbacks, and the Climate Benefits of Forests. *Science*, 320(5882):1444–1449.

Bourg, N. A., McShea, W. J., Thompson, J. R., McGarvey, J. C., and Shen, X. (2013). Initial census, woody seedling, seed rain, and stand structure data for the SCBI SIGEO Large Forest Dynamics Plot. *Ecology*, 94(9):2111–2112.

Bretfeld, M., Ewers, B. E., and Hall, J. S. (2018). Plant water use responses along secondary forest succession during the 2015–2016 El Niño drought in Panama. *New Phytologist*, 219(3):885–899.

Clark, J. S., Iverson, L., Woodall, C. W., Allen, C. D., Bell, D. M., Bragg, D. C., D'Amato, A. W., Davis, F. W., Hersh, M. H., Ibanez, I., Jackson, S. T., Matthews, S., Pederson, N., Peters, M., Schwartz, M. W.,

Waring, K. M., and Zimmermann, N. E. (2016). The impacts of increasing drought on forest dynamics, structure, and biodiversity in the United States. *Global Change Biology*, 22(7):2329–2352.

Condit, R. (1998). *Tropical Forest Census Plots: Methods and Results from Barro Colorado Island, Panama and a Comparison with Other Plots*. Springer Berlin Heidelberg, Berlin, Heidelberg.

Couvreur, V., Ledder, G., Manzoni, S., Way, D. A., Muller, E. B., and Russo, S. E. (2018). Water transport through tall trees: A vertically explicit, analytical model of xylem hydraulic conductance in stems. *Plant, Cell & Environment*, 41(8):1821–1839.

D'Orangeville, L., Maxwell, J., Kneeshaw, D., Pederson, N., Duchesne, L., Logan, T., Houle, D., Arseneault, D., Beier, C. M., Bishop, D. A., Druckenbrod, D., Fraver, S., Girard, F., Halman, J., Hansen, C., Hart, J. L., Hartmann, H., Kaye, M., Leblanc, D., Manzoni, S., Ouimet, R., Rayback, S., Rollinson, C. R., and Phillips, R. P. (2018). Drought timing and local climate determine the sensitivity of eastern temperate forests to drought. *Global Change Biology*, 24(6):2339–2351.

Druckenbrod, D. L., Martin-Benito, D., Orwig, D. A., Pederson, N., Poulter, B., Renwick, K. M., and Shugart, H. H. (2019). Redefining temperate forest responses to climate and disturbance in the eastern United States: New insights at the mesoscale. *Global Ecology and Biogeography*, 28(5):557–575.

Elliott, K. J., Miniat, C. F., Pederson, N., and Laseter, S. H. (2015). Forest tree growth response to hydroclimate variability in the southern Appalachians. *Global Change Biology*, 21(12):4627–4641.

Friedlingstein, P., Cox, P., Betts, R., Bopp, L., von Bloh, W., Brovkin, V., Cadule, P., Doney, S., Eby, M., Fung, I., Bala, G., John, J., Jones, C., Joos, F., Kato, T., Kawamiya, M., Knorr, W., Lindsay, K., Matthews, H. D., Raddatz, T., Rayner, P., Reick, C., Roeckner, E., Schnitzler, K.-G., Schnur, R., Strassmann, K., Weaver, A. J., Yoshikawa, C., and Zeng, N. (2006). Climate–Carbon Cycle Feedback Analysis: Results from the C4mip Model Intercomparison. *Journal of Climate*, 19(14):3337–3353.

Friedrichs, D. A., Trouet, V., Büntgen, U., Frank, D. C., Esper, J., Neuwirth, B., and Löffler, J. (2009). Species-specific climate sensitivity of tree growth in Central-West Germany. *Trees*, 23(4):729.

Gonzalez-Akre, E., Meakem, V., Eng, C.-Y., Tepley, A. J., Bourg, N. A., McShea, W., Davies, S. J., and Anderson-Teixeira, K. (2016). Patterns of tree mortality in a temperate deciduous forest derived from a large forest dynamics plot. *Ecosphere*, 7(12):e01595.

Greenwood, S., Ruiz-Benito, P., Martínez-Vilalta, J., Lloret, F., Kitzberger, T., Allen, C. D., Fensham, R., Laughlin, D. C., Kattge, J., Bönisch, G., Kraft, N. J. B., and Jump, A. S. (2017). Tree mortality across biomes is promoted by drought intensity, lower wood density and higher specific leaf area. *Ecology Letters*, 20(4):539–553.

Guerfel, M., Baccouri, O., Boujnah, D., Chaïbi, W., and Zarrouk, M. (2009). Impacts of water stress on gas exchange, water relations, chlorophyll content and leaf structure in the two main Tunisian olive (Olea europaea L.) cultivars. *Scientia Horticulturae*, 119(3):257–263.

Hacket-Pain, A. J., Cavin, L., Friend, A. D., and Jump, A. S. (2016). Consistent limitation of growth by high temperature and low precipitation from range core to southern edge of European beech indicates widespread vulnerability to changing climate. *European Journal of Forest Research*, 135(5):897–909.

Harris, I., Jones, P. D., Osborn, T. J., and Lister, D. H. (2014). Updated high-resolution grids of monthly climatic observations – the CRU TS3.10 Dataset. *International Journal of Climatology*, 34(3):623–642.

Helcoski, R., Tepley, A. J., Pederson, N., McGarvey, J. C., Meakem, V., Herrmann, V., Thompson, J. R., and Anderson-Teixeira, K. J. (2019). Growing season moisture drives interannual variation in woody productivity of a temperate deciduous forest. *New Phytologist*, 0(0).

Hoffmann, W. A., Marchin, R. M., Abit, P., and Lau, O. L. (2011). Hydraulic failure and tree dieback are associated with high wood density in a temperate forest under extreme drought. *Global Change Biology*, 17(8):2731–2742.

Intergovernmental Panel on Climate Change (2015). *Climate Change 2014: Impacts, Adaptation and Vulnerability: Working Group II Contribution to the IPCC Fifth Assessment Report. Volume 2 Volume 2*. OCLC: 900892773.

Jennings, S. B., Brown, N. D., and Sheil, D. (1999). Assessing forest canopies and understorey illumination: canopy closure, canopy cover and other measures. *Forestry: An International Journal of Forest Research*, 72(1):59–74.

Kannenberg, S. A., Novick, K. A., Alexander, M. R., Maxwell, J. T., Moore, D. J. P., Phillips, R. P., and Anderegg, W. R. L. (2019). Linking drought legacy effects across scales: From leaves to tree rings to ecosystems. *Global Change Biology*, 0(ja).

Kennedy, D., Swenson, S., Oleson, K. W., Lawrence, D. M., Fisher, R., Costa, A. C. L. d., and Gentine, P. (2019). Implementing Plant Hydraulics in the Community Land Model, Version 5. *Journal of Advances in Modeling Earth Systems*, 11(2):485–513.

Koike, T., Kitao, M., Maruyama, Y., Mori, S., and Lei, T. T. (2001). Leaf morphology and photosynthetic adjustments among deciduous broad-leaved trees within the vertical canopy profile. *Tree Physiology*, 21(12-13):951–958.

Kunert, N., Aparecido, L. M. T., Wolff, S., Higuchi, N., Santos, J. d., Araujo, A. C. d., and Trumbore, S. (2017). A revised hydrological model for the Central Amazon: The importance of emergent canopy trees in the forest water budget. *Agricultural and Forest Meteorology*, 239:47–57.

Larjavaara, M. and Muller-Landau, H. C. (2013). Measuring tree height: a quantitative comparison of two common field methods in a moist tropical forest. *Methods in Ecology and Evolution*, 4(9):793–801.

Liu, H., Gleason, S. M., Hao, G., Hua, L., He, P., Goldstein, G., and Ye, Q. (2019). Hydraulic traits are coordinated with maximum plant height at the global scale. *Science Advances*, 5(2):eaav1332.

Liu, Y. and Muller, R. N. (1993). Effect of Drought and Frost on Radial Growth of Overstory and Undesrstory Stems in a Deciduous Forest. *The American Midland Naturalist*, 129(1):19–25.

Lloret, F., Keeling, E. G., and Sala, A. (2011). Components of tree resilience: effects of successive low-growth episodes in old ponderosa pine forests. *Oikos*, 120(12):1909–1920.

Maréchaux, I., Bartlett, M. K., Sack, L., Baraloto, C., Engel, J., Joetzjer, E., and Chave, J. (2015). Drought tolerance as predicted by leaf water potential at turgor loss point varies strongly across species within an Amazonian forest. *Functional Ecology*, 29(10):1268–1277.

McDowell, N. G. and Allen, C. D. (2015). Darcy's law predicts widespread forest mortality under climate warming. *Nature Climate Change*, 5(7):669–672.

McDowell, N. G., Bond, B. J., Dickman, L. T., Ryan, M. G., and Whitehead, D. (2011). Relationships Between Tree Height and Carbon Isotope Discrimination. In Meinzer, F. C., Lachenbruch, B., and Dawson, T. E., editors, *Size- and Age-Related Changes in Tree Structure and Function*, Tree Physiology, pages 255–286. Springer Netherlands, Dordrecht.

Meakem, V., Tepley, A. J., Gonzalez-Akre, E. B., Herrmann, V., Muller-Landau, H. C., Wright, S. J., Hubbell, S. P., Condit, R., and Anderson-Teixeira, K. J. (2018). Role of tree size in moist tropical forest carbon cycling and water deficit responses. *New Phytologist*, 219(3):947–958.

Medeiros, C. D., Scoffoni, C., John, G. P., Bartlett, M. K., Inman-Narahari, F., Ostertag, R., Cordell, S., Giardina, C., and Sack, L. (2019). An extensive suite of functional traits distinguishes Hawaiian wet and dry forests and enables prediction of species vital rates. *Functional Ecology*, 33(4):712–734.

Muller-Landau, H. C., Condit, R. S., Chave, J., Thomas, S. C., Bohlman, S. A., Bunyavejchewin, S., Davies, S., Foster, R., Gunatilleke, S., Gunatilleke, N., Harms, K. E., Hart, T., Hubbell, S. P., Itoh, A., Kassim, A. R., LaFrankie, J. V., Lee, H. S., Losos, E., Makana, J.-R., Ohkubo, T., Sukumar, R., Sun, I.-F., Nur Supardi, M. N., Tan, S., Thompson, J., Valencia, R., Muñoz, G. V., Wills, C., Yamakura, T., Chuyong, G., Dattaraja, H. S., Esufali, S., Hall, P., Hernandez, C., Kenfack, D., Kiratiprayoon, S., Suresh, H. S., Thomas, D., Vallejo, M. I., and Ashton, P. (2006). Testing metabolic ecology theory for allometric scaling of tree size, growth and mortality in tropical forests. *Ecology Letters*, 9(5):575–588.

NEON (2018). National Ecological Observatory Network. 2016, 2017, 2018. Data Products: DP1.00001.001, DP1.00098.001, DP1.00002.001. Provisional data downloaded from http://data.neonscience.org/ in May 2019. Battelle, Boulder, CO, USA.

Olson, M. E., Soriano, D., Rosell, J. A., Anfodillo, T., Donoghue, M. J., Edwards, E. J., León-Gómez, C., Dawson, T., Martínez, J. J. C., Castorena, M., Echeverría, A., Espinosa, C. I., Fajardo, A., Gazol, A., Isnard, S., Lima, R. S., Marcati, C. R., and Méndez-Alonzo, R. (2018). Plant height and hydraulic vulnerability to drought and cold. *Proceedings of the National Academy of Sciences*, 115(29):7551–7556.

Pretzsch, H., Schütze, G., and Biber, P. (2018). Drought can favour the growth of small in relation to tall trees in mature stands of Norway spruce and European beech. *Forest Ecosystems*, 5(1):20.

R Core Team (2019). *R: A Language and Environment for Statistical Computing*. R Foundation for Statistical Computing, Vienna, Austria.

Rodríguez-Catón, M., Villalba, R., Srur, A. M., and Luckman, B. (2015). Long-term trends in radial growth associated with Nothofagus pumilio forest decline in Patagonia: Integrating local- into regional-scale patterns. *Forest Ecology and Management*, 339:44–56.

Roskilly, B., Keeling, E., Hood, S., Giuggiola, A., and Sala, A. (2019). Conflicting functional effects of xylem pit structure relate to the growth-longevity trade-off in a conifer species. *PNAS. doi: /10.1073/pnas.1900734116.*

Ryan, M. G., Phillips, N., and Bond, B. J. (2006). The hydraulic limitation hypothesis revisited. *Plant, Cell & Environment*, 29(3):367–381.

Scharnweber, T., Heinze, L., Cruz-García, R., van der Maaten-Theunissen, M., and Wilmking, M. (2019). Confessions of solitary oaks: We grow fast but we fear the drought. *Dendrochronologia*, 55:43–49.

Schöngart, J., Bräuning, A., Barbosa, A. C. M. C., Lisi, C. S., and de Oliveira, J. M. (2017). Dendroecological Studies in the Neotropics: History, Status and Future Challenges. In Amoroso, M. M., Daniels, L. D., Baker, P. J., and Camarero, J. J., editors, *Dendroecology: Tree-Ring Analyses Applied to Ecological Studies*, Ecological Studies, pages 35–73. Springer International Publishing, Cham.

Scoffoni, C., Vuong, C., Diep, S., Cochard, H., and Sack, L. (2014). Leaf Shrinkage with Dehydration: Coordination with Hydraulic Vulnerability and Drought Tolerance. *Plant Physiology*, 164(4):1772–1788.

Simeone, C., Maneta, M. P., Holden, Z. A., Sapes, G., Sala, A., and Dobrowski, S. Z. (2019). Coupled ecohydrology and plant hydraulics modeling predicts ponderosa pine seedling mortality and lower treeline in the US Northern Rocky Mountains. *New Phytologist*, 221(4):1814–1830.

Slette, I. J., Post, A. K., Awad, M., Even, T., Punzalan, A., Williams, S., Smith, M. D., and Knapp, A. K. (2019). How ecologists define drought, and why we should do better. *Global Change Biology*, 0(0):1–8.

Smith, W. K. and Nobel, P. S. (1977). Temperature and Water Relations for Sun and Shade Leaves of a Desert Broadleaf, Hyptis emoryi. *Journal of Experimental Botany*, 28(1):169–183.

Stovall, A. E. L., Anderson-Teixeira, K. J., and Shugart, H. H. (2018a). Assessing terrestrial laser scanning for developing non-destructive biomass allometry. *Forest Ecology and Management*, 427:217–229.

Stovall, A. E. L., Anderson-Teixeira, K. J., and Shugart, H. H. (2018b). Terrestrial LiDAR-derived non-destructive woody biomass estimates for 10 hardwood species in Virginia. *Data in Brief*, 19:1560–1569.

Stovall, A. E. L., Shugart, H., and Yang, X. (2019). Tree height explains mortality risk during an intense drought. *Nature Communications*, 10(1):1–6.

Suarez, M. L., Ghermandi, L., and Kitzberger, T. (2004). Factors predisposing episodic drought-induced tree mortality in Nothofagus– site, climatic sensitivity and growth trends. *Journal of Ecology*, 92(6):954–966.

Sørensen, R., Zinko, U., and Seibert, J. (2006). On the calculation of the topographic wetness index: evaluation of different methods based on field observations. *Hydrology and Earth System Sciences*, 10(1):101–112.

Trenberth, K. E., Dai, A., van der Schrier, G., Jones, P. D., Barichivich, J., Briffa, K. R., and Sheffield, J. (2014). Global warming and changes in drought. *Nature Climate Change*, 4(1):17–22.

Twery, M. J. (1991). Effects of defoliation by gypsy moth. *IN: Gottschalk, Kurt W.; Twery, Mark J.; Smith, Shirley I., eds. Proceedings, U.S. Department of Agriculture interagency gypsy moth research review 1990; East Windsor, CT. Gen. Tech. Rep. NE-146. Radnor, PA: U.S. Department of Agriculture, Forest Service, Northeastern Forest Experiment Station. 27-39.*, 146.

Zuleta, D., Duque, A., Cardenas, D., Muller-Landau, H. C., and Davies, S. J. (2017). Drought-induced mortality patterns and rapid biomass recovery in a terra firme forest in the Colombian Amazon. *Ecology*, 98(10):2538–2546.

Table 1. Summary of hypotheses, corresponding specific predictions, and results. We count predictions as fully supported ('yes') when the response is signficant in single-variable tests (Table 4) and included in all top full models and as partially supported ('(yes)') or rejected ('(no)') when the direction of response consistently matched the prediction but the effect was not significant in all models.

	Prediction supported?				
Hypotheses & Specific Predictions	Overall	1966	1977	1999	Results
Tree size and microenvironment					
Larger, taller trees have lower Rt.					
Rt decreases with stem diameter (DBH).	yes	yes	-	-	Table 4
Rt decreases with height (H).	yes	yes	-	(yes)	Tables 4, 5
Trees with more exposed crowns have lower Rt.					
Dominant trees have lowest Rt.	-	yes	(yes)	-	Tables 4, 5
Correcting for H, dominant trees have lowest Rt.	(no)		-	(no)	Tables 4, 5
Small trees (lower root volume) in drier microhabitats have lower Rt.					
There is a negative interactive effect between H and topographic wetness index.	-	-	-	-	Table 4
Species traits					
Species' traits–particularly leaf hydraulic traits–predict Rt.					
Wood density correlates (positively or negatively) to Rt.	-	-	-	-	Table 4
Leaf mass per area correlates positively to Rt.	-	-	-	-	Table 4
Ring-porous species have higher Rt than diffuse- or semi-ring- porous.	-	yes	(no)	yes	Tables 4, 5
Percent loss leaf area upon desiccation correlates negatively with Rt.	yes	yes	(yes)	-	Tables 4, 5
Water potential at turgor loss correlates negatively with Rt.	(yes)	-	(yes)	(yes)	Tables 4, 5

Table 2. Summary of variables.

variable	symbol	units	description	category	n
Dependent variable					
drought resistance	Rt	-	ratio of growth during drought year to mean growth of the 5 years prior.	-	1596
Independent variables					
drought year	Y	-	year of drought	1966	478
				1977	547
				1999	571
tree size					
diameter breast height	DBH	cm	DBH in drought year	-	all
height	H	m	estimated H in drought year	-	all
microhabitat					
crown position	CP	-	2018 crown position	dominant (D)	31
				co-dominant (C)	231
				intermediate (I)	224
				suppressed (S)	101
topographic wetness index	TWI	-	steady-state wetness index based on slope and upstream contributing area	-	all
species' traits					
wood density	WD	g cm^{-3}	dry mass of a unit volume of fresh wood	-	all
leaf mass per area	LMA	kg m^{-2}	ratio of leaf dry mass to fresh leaf area	-	all
xylem porosity	XP	-	vessel arrangement in xylem	ring (R)	408
				semi-ring (SR)	31
				diffuse (D)	178
turgor loss point	π_{tlp}	MPa	water potential at which leaves wilt	-	all
percent loss area	PLA_{dry}	%	percent loss of leaf area upon dessication	-	all

Table 3. Overview of analyzed species, their productivity in the plot, numbers and sizes sampled, and traits. Given are DBH mean and range of cored trees, the number of cores represented by each crown position of each species, and mean hydraulic trait measurements.

species	percent.ANPP	n.cores	mean.DBH_cm	DBH.range_cm	WD_g.per.cm3	LMA_g.per.cm2	xylem.porosity	TLP_Mpa	PLA_percent
Liriodendron tulipifera	47.1	109	36.9	90.4	0.40	46.92	diffuse	-1.92	19.56
Quercus alba	10.7	66	47.2	67.7	0.61	75.80	ring	-2.58	8.52
Quercus rubra	10.1	71	54.9	136.9	0.62	71.13	ring	-2.64	11.01
Quercus velutina	7.8	83	54.1	98.2	0.65	48.69	ring	-2.39	13.42
Quercus montana	4.8	67	42.2	76.7	0.61	71.77	ring	-2.36	11.75
Fraxinus americana	3.8	69	35.4	88.3	0.56	43.28	ring	-2.10	13.06
Carya glabra	3.7	39	31.4	88.7	0.62	42.76	ring	-2.13	21.09
Juglans nigra	2.1	31	48.1	62.8	1.09	72.13	semi-ring*	-2.76	24.64
Carya cordiformis	2.0	17	27.2	50.8	0.83	45.86	ring	-2.13	17.22
Carya tomentosa	2.0	18	21.0	20.1	0.83	45.36	ring	-2.20	16.56
Fagus grandifolia	1.5	81	23.5	96.0	0.62	30.68	diffuse	-2.57	9.45
Carya ovalis	1.1	24	35.3	51.1	0.96	47.60	ring	-2.48	14.80

*Semi-ring porosity is intermediate between ring and diffuse. We group it with diffuse-porous species for more even division of species between categories.

Table 4. Single-variable tests of hypothesized drivers of drought resistance. Models including each variable were compared to corresponding null models. dAIC is the AICc of the null model minus that of the model including the variable (thus, dAICc>2 indicates that the variable significantly improves the model

			all droughts		1966		1977		1999	
variable	category	null model variables	dAICc	coefficients	dAICc	coefficients	dAICc	coefficients	dAICc	coefficients
Tree size and microenvironment										
ln[DBH]		(year)	8.17**	-0.0385	15.32**	-0.0888	-0.87	-0.0214	-1.93	0.0057
ln[H]		(year)	8.17**	-0.0600	15.32**	-0.1383	-0.87	-0.0334	-1.93	0.0089
crown position	D	(year)	-2.96	-0.0461	3.25**	-0.0509	0.66	-0.0759	0.38	-0.0103
(alone)	C		-	0.0000	-	0.0000	-	0.0000	-	0.0000
	I		-	-0.0063	-	0.0732	-	-0.0298	-	-0.0563
	S		-	0.0122	-	0.0526	-	0.0432	-	-0.0483
crown position	D	ln[H] (+year)	0.57	-0.0347	-1.84	-0.0328	-0.23	-0.0730	3.04**	-0.0024
(with height)	C		-	0.0000	-	0.0000	-	0.0000	-	0.0000
	I		-	-0.0425	-	0.0139	-	-0.0388	-	-0.0810
	S		-	-0.0582	-	-0.0662	-	0.0258	-	-0.0956
ln[TWI]		ln[H] (+year)	5.34**	-0.0890	-1.96	-0.0171	5.05**	-0.1404	2.8**	-0.1033
ln[TWI]*ln[H]		ln[H]+ln[TWI] (+year)	-0.83	0.0797	-1.58	0.0927	-1.47	0.0861	-1.9	0.0414
Species traits										
wood density		ln[H] (+year)	-1.91	-0.0479	-1.24	-0.2089	-1.22	-0.1812	0.22	0.2502
leaf mass per area		ln[H] (+year)	-1.99	0.0003	-1.88	0.0012	-1.76	-0.0013	-2	0.0004
xylem porosity	R	ln[H] (+year)	-0.71	0.0660	2.305**	0.1888	1.399*	-0.1452	3.765**	0.1544
	D/SR		-	0.0000	-	0.0000	-	0.0000	-	0.0000
turgor loss point		ln[H] (+year)	1.33*	-0.1777	-1.64	-0.1078	1.26*	-0.2500	0.016	-0.1732
percent loss area		ln[H] (+year)	7.17**	-0.0140	9.18**	-0.0249	-0.05	-0.0105	-0.716	-0.0074

*dAICc > 1: variable qualified for inclusion in full model

**dAICc > 2: statistically signficant, variable qualified for inclusion in full model

Table 5. Summary of top full models for each drought instance. Models are ranked by AICc, and we show all models whose AICc value falls within 1.0 (dAICc<1) of the best model (bold).

					crown position					xylem architecture			
drought	dAICc	R2	Intercept	ln[H]	D	C	I	S	ln[TWI]	D/SR	R	PLA	TLP
all	**0.000**	**0.12**	**1.077**	**-0.057**	**-**	**-**	**-**	**-**	**-0.086**	**-**	**-**	**-0.012**	**-0.113**
	0.586	0.11	1.365	-0.055	-	-	-	-	-0.086	-	-	-0.013	-
	0.726	0.12	1.220	-0.089	-0.034	0	-0.037	-0.051	-0.079	-	-	-0.012	-0.101
	0.813	0.11	1.481	-0.089	-0.034	0	-0.039	-0.054	-0.079	-	-	-0.014	-
1966	**0.000**	**0.25**	**1.503**	**-0.141**	**-**	**-**	**-**	**-**	**-**	**0**	**0.11**	**-0.021**	**-**
1977	**0.000**	**0.21**	**1.136**	**-**	**-**	**-**	**-**	**-**	**-0.145**	**0**	**-0.205**	**-0.015**	**-0.13**
	0.040	0.21	1.490	-	-	-	-	-	-0.145	0	-0.22	-0.017	-
	0.505	0.22	1.089	-	-0.069	0	-0.025	0.043	-0.137	0	-0.199	-0.014	-0.143
	0.818	0.22	1.481	-	-0.07	0	-0.027	0.038	-0.136	0	-0.216	-0.017	-
1999	**0.000**	**0.23**	**0.464**	**-**	**-**	**-**	**-**	**-**	**-0.095**	**0**	**0.16**	**-**	**-0.197**
	0.019	0.24	0.725	-0.068	0	0	-0.077	-0.09	-0.084	0	0.167	-	-0.183

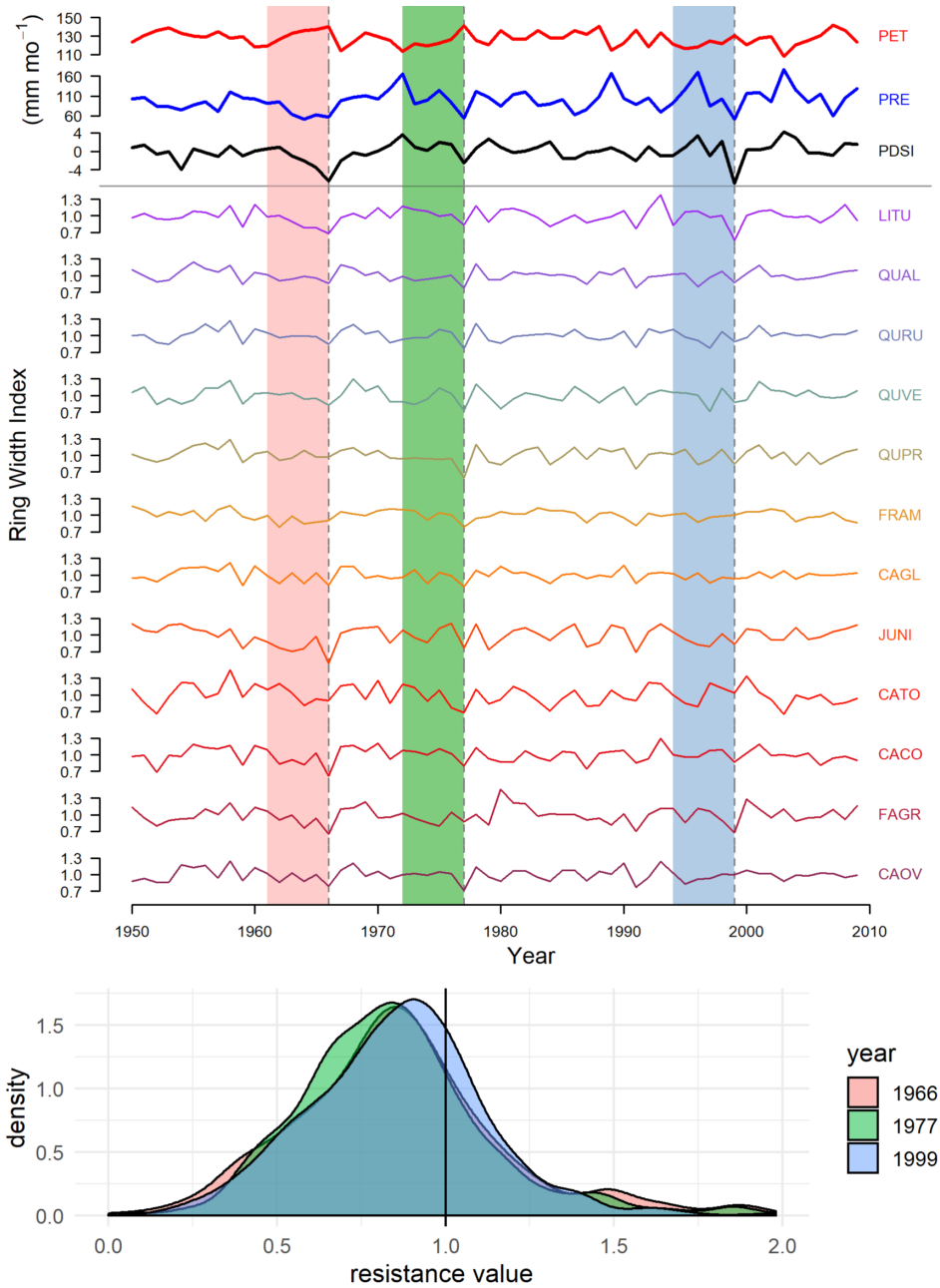

Figure 1. Climate and species-level growth responses over our study period, highlighting the three focal drougths (a) and community-wide responses Time series plot (a) shows peak growing season (May-August) climate conditions and residual chronologies for each species. Focal droughts are indicated by dashed lines, and shading indicates the pre-drought period used in calculations of the resistance metric. Figure modified from Helcoski *et al.* (2019). Density plots (b) show the distribution of resistance values for each drought.

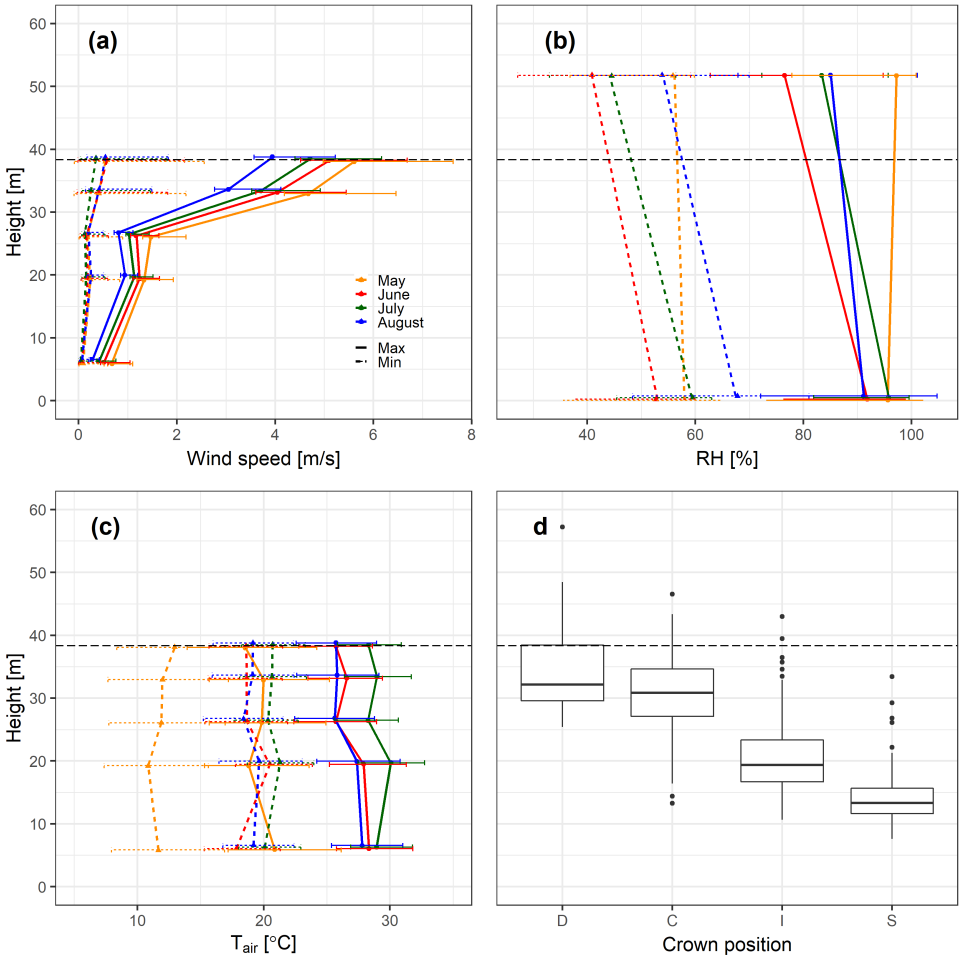

Figure 2. Height profiles in growing season climatic conditions, tree heights by crown position, and leaf hydraulic traits The top row shows averages (± SD) of daily maxima and minima of (a) wind speed, (b) relative humidity (RH), and (c) air temperature (T_{air}) averaged over each month of the peak growing season (May-August) from 2016-2018. In these plots, heights are slightly offset for visualization purposes. Also shown is (d) 2018 tree heights by canopy position (see Table 2 for codes). In all plots, the dashed horizontal line indicates the 95th percentile of tree heigts in the ForestGEO plot.